# CHT and TTT Curing Diagrams of Polyflavonoid Tannin Resins

**S. GARNIER, A. PIZZI**

ENSTIB, University of Nancy 1, 88051 Epinal, France

*Received 29 February 2000; accepted 18 November 2000*

**ABSTRACT:** TTT and CHT curing diagrams for tannin-based adhesives were built by thermomechanical analysis (TMA) by following the *in situ* hardening directly in a wood joint, and the curve trends observed were similar to those previously observed for synthetic polycondensation resins on lignocellulosic substrates. Of the parameters that most influence the relative position of vitrification and gel curves on the diagrams (i.e., where the influence has been quantified), chief among them is the reactivity of the tannin with formaldehyde and any factor influencing it: thus, the inherent higher reactivity of the A-ring of the tannin (such as in procyanidins versus prorobinetinidins) and the pH of the tannin solution. The percentage formaldehyde hardener has some influence in CHT diagrams, especially for the slower-reacting tannins, but practically no influence in TTT diagrams within the 4–10% formaldehyde range used. As in the case of synthetic polycondensation adhesive resins, regression equations relating the internal bond strength of a wood particleboard, prepared under controlled conditions, with the inverse of the minimum deflection, obtained by constant heating rate TMA of a wood joint during resin cure, have been obtained for the two types of tannins of lower reactivity (profisetinidins/prorobinetinidins) but not for the faster-reacting procyanidin and prodelphinidin tannins. © 2001 John Wiley & Sons, Inc. J Appl Polym Sci 81: 3220–3230, 2001

## INTRODUCTION

The concept of the isothermal time–temperature–transformation (TTT) cure diagram, in which gelation and vitrification times are plotted versus the isothermal cure temperature, is useful for understanding the behavior of thermosetting resins under isothermal cure conditions.[1] Analogous to the isothermal TTT diagram is the continuous heating transformation (CHT) cure diagram, which reports the times and temperatures required to reach similar events during the course of continuous heating at constant heating rates.[2] The gelation and vitrification curves are the most characteristic features of both TTT and CHT diagrams; the S-shape of the CHT diagram, in particular, defines the region at which the reaction rate is greatly reduced because diffusion control becomes more pronounced in the glass-transition region. Although the majority of the CHT and TTT diagrams studies reported to date have mostly focused on the curing of epoxy resins on glass fiber braid,[1–5] CHT and TTT diagrams of other polycondensation resins used in considerable amounts as wood adhesives [i.e., urea–formaldehyde (UF), melamine–urea–formaldehyde (MUF) resins, phenol–formaldehyde (PF), and phenol–resorcinol–formaldehyde (PRF) cold-set resins, on lignocellulosic substrates (i.e., wood)] have recently been reported.[6,7] Such studies have been carried out because these resins are the most used (by volume) polycondensation resins to

*Correspondence to:* A. Pizzi (pizzi@enstib.u-nancy.fr).

Journal of Applied Polymer Science, Vol. 81, 3220–3230 (2001)

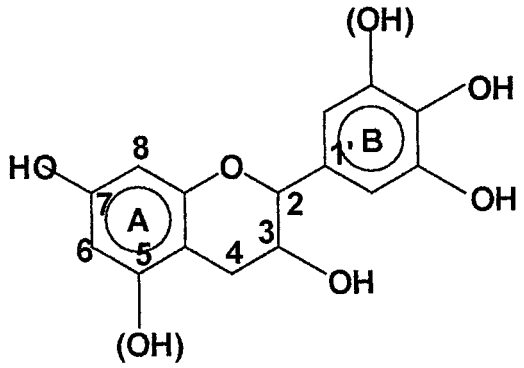


**Scheme 1**

date, of which their main use is as thermosetting wood adhesives.[8] The presence of the lignocellulosic substrate and the fact that the resins are in water solution yielded CHT diagrams rather different from the CHT diagrams reported for epoxy resins in the absence of water and on a nonreactive substrate such as glass.[8]

Polyflavonoid tannins are natural polyphenolic materials that can be hardened by reaction with formaldehyde.[8] They have also been used for over 20 years as industrial thermosetting tannin–formaldehyde adhesives for wood products.[8] Their resin technology and application are very different from those of synthetic PF resins because of their much greater reactivity toward formaldehyde.[8] Industrial polyflavonoid tannin extracts are primarily composed of flavan-3-ol repeating units, linked 4–6 and 4–8, and smaller fractions of polysaccharides and simple sugars. Two types of phenolic rings with different reactivities with formaldehyde are present on each flavan-3-ol repeating unit, that is, A-rings and B-rings, although the A-rings are those on which the reaction and hardening of polyflavonoid tannins with formaldehyde are based. Compared to the relative reactivity of phenol with formaldehyde taken as 1, the reactivity of the A-ring of profisetinidin/prorobinetinidin-type tannins with formaldehyde is approximately 7–8, whereas the reactivity of the A-rings of procyanidin/prodelphinidin-type tannins is 35–40. For this reason formaldehyde, in a much lesser proportion than that in synthetic resins, is used here only as a hardener; the tannin does not need to be built up to oligomers. The resin pH is a parameter of fundamental importance in these thermosetting resins, with regard to resin reactivity and performance, and so is the A-ring structure of the flavonoid repeating unit, as shown in Scheme 1.

This study presents the CHT and TTT diagrams obtained by TMA for these types of resins on a standard wood substrate (beech wood) in the high-temperature zone of the two types of diagram. The variations induced on the relative position of gel and vitrification curves in the diagrams resulting from (1) the variation of resin : aldehyde molar ratio (herewith limited to just the variation of the percentage formaldehyde hardener) and (2) the variation of pH in relation to the A-ring reactivity of the different tannins are also studied.

## EXPERIMENTAL

### Thermomechanical Analysis (TMA) Determination of TTT and CHT Curing Diagrams

Recently, work on the formation of polymer networks by photopolymerizable and polyester surface finishes on wood and of polycondensation resins used as wood adhesives has yielded a mathematical relationship[9–11] between the energy of interaction ($E$) at the synthetic polymer/wood interface calculated by molecular mechanics (work of adhesion), the number of degrees of freedom ($m$) of the segment of the synthetic polymer between two crosslinking nodes, the coefficient of branching (hence the functionality of the starting monomer), and the relative deflection ($f$) obtained by thermomechanical analysis (TMA) of wood specimens coated or bonded with the adhesive. The relationship is expressed by $f = km/E$, where $k$ is a constant.[9–11] Regression equations[9] directly correlating $m$ with $E$ and $m$ with $f$ have been derived for hardened phenol–formaldehyde (PF), resorcinol–formaldehyde (RF), melamine–formaldehyde (MF), and tannin–formaldehyde (TF) resins. These relationships can be used, by thermomechanical analysis, to follow the hardening of a thermosetting adhesive directly in the wood joint. The classical mechanics relation between force and deflection $E = [L^3/(4bh^3)][\Delta F/\Delta f]$ allows the calculation of the Young's modulus $E$ for each of the cases tested. Because the deflections $\Delta f$ obtained were proved to be constant and reproducible,[8–10] and because they are proportional to the flexibility of the assembly, the relative flexibility as expressed by the Young's modulus of the two primers can be calculated for the two finishes through the relationship $E_1/E_2 = \Delta f_2/\Delta f_1$. The values of Young's modulus for the resins/substrates

systems were then calculated according to previously reported methods according to the equation $f = km/\alpha E$ and connected regression equations, which were also previously reported.[9]

To this purpose tannin–paraformaldehyde resins based on the two profisetinidin/prorobinetinidin-type commercial tannin extracts from the bark of mimosa (*Acacia mearnsii ex* Tanac, Brazil) and from the wood of quebracho (*Schinopsis balansae ex* Indunor, Argentina) were tested dynamically by thermomechanical analysis (TMA) on a Mettler 40 (Switzerland) apparatus. The mimosa extract was used as obtained without modifying it to an adhesive intermediate,[8] whereas the quebracho extract was the commercial adhesive intermediate, that is, a tannin extract modified by an already published procedure of acid and basic hydrolysis. A commercial procyanidin tannin extract from the bark of pine (*Pinus radiata ex* Diteco, Chile) and a commercial pecan nut (*Carya illinoensis*) membrane tannin extract were also tested. Water solutions of the tannin extracts at concentrations between 35 and 45% in water were tested first at their natural pH of extraction, which was 4.2 for mimosa, 4.8 for pine, and 5.1 for both quebracho and pecan tannin extracts. The pH of two extracts, mimosa and pine, were also varied to test solutions at pH 7 and pH 9, while maintaining constant at 4 wt % on tannin extract solids the proportion of fine paraformaldehyde powder hardener used.

Variations of the amount of paraformaldehyde hardener were also carried out, and the TTT and CHT diagrams for the same tannins were constructed for, respectively, 2, 4, 8, and 10 wt % paraformaldehyde hardener on tannin extract solids. Samples of beech wood alone and of two beech wood plies bonded with each system of liquid polycondensate resins in a layer of 350 $\mu$m, for a total sample dimension of 21 $\times$ 6 $\times$ 1.1 mm were tested: (1) for the CHT diagrams in nonisothermal mode between 20 and 450°C at heating rates of 5, 7.5, 10, 15, 20, 25, 30, 40, 50, 60, and 70°C/min; and (2) for the TTT diagrams by heating at a constant heating rate to a predetermined temperature and then maintaining the joints under isothermal conditions (final temperatures were initially 25, 40, 60, 80, 100, 120, 140, 160, 180, 200, and 225°C, as indicated in the figures), with a Mettler 40 TMA apparatus in three-point bending on a span of 18 mm, exercising a force cycle of 0.1 N/0.5 N on the specimens with each force cycle of 12 s (6 s/6 s), and the resulting modulus curves as a function of both temperature and time were obtained. Gel and start and total vitrification were identified on the TMA curves of modulus versus temperature and modulus versus time according to procedures previously reported.[12,13] The diagrams were built according to the approximation of Pascault and Williams according to $T_{cure} = T_g$.[14]

Four tannin extract–formaldehyde mixes for nonmodified mimosa tannin, modified quebracho tannin, nonmodified pine tannin, and nonmodified pecan nut tannin, respectively, in which all the formaldehyde was added as paraformaldehyde fine powder in the mix at the levels of 2, 4, 8, and 10 wt %, respectively, were prepared according to previously reported procedures.[8] The resins were then tested by thermomechanical analysis (TMA), according to procedures reported in the lierature,[9–11,15,16] by placing 30 mg of resin between two plies of beech wood to form a joint of 21 $\times$ 6 $\times$ 14 mm dimension tested in three-point bending for a span of 18 mm, subjected to an alternating force of 0.1 N/0.5 N with a 6 s/6 s cycle at a constant heating rate of 10°C/min, from 40 to 250°C. The minimum value of the deflection corresponding to the tighter network formed by the adhesive in the wood joint was then measured. Because the resins had different solids contents the TMA values were corrected for adhesive quantity in the joint. Duplicate one-layer laboratory particleboards of 350 $\times$ 310 $\times$ 14 mm dimensions were then produced by adding 10 wt % tannin resin solids content on dry wood particles pressed at a maximum pressure of 28 kg/cm$^2$, followed by a descending pressing cycle, at 195°C, for a pressing time of 8 min to ensure complete curing. All the panels had densities between 0.680 and 0.695 g/cm$^3$. After light surface sanding the panels were tested for dry internal bond (IB) strength. The results obtained are shown in Table I.

## DISCUSSION

Trends different from those reported in the literature for TTT and CHT diagrams of epoxy resins occur in the high-temperature zone of the diagrams of water-borne formaldehyde-based resins hardening on lignocellulosic substrates. This was previously reported for synthetic polycondensation resins (UF, MUF, PF, PRF). This is also the case for tannin–formaldehyde resins but with the added complication that, although different tannin structures correspond to similar curing dia-

**Table I TMA Deflection Values and Wood Particleboard Internal Bond (IB) Strengths Obtained for Different Tannins When Varying the Weight Percentage of Paraformaldehyde Hardener**

| | Paraformaldehyde Hardener | | | |
|---|---|---|---|---|
| Tannin Extract | 4 wt % | 6 wt % | 8 wt % | 10 wt % |
| Mimosa tannin | | | | |
| Dry IB strength (MPa) | 0.46 | 0.57 | 0.68 | 0.79 |
| TMA deflection ($\mu$m) | 16.1 | 15.8 | 15.7 | 14.4 |
| Quebracho tannin | | | | |
| Dry IB strength (MPa) | 0.37 | 0.46 | 0.54 | 0.63 |
| TMA deflection ($\mu$m) | 26.8 | 22.1 | 18.3 | 17.4 |
| Pecan tannin | | | | |
| Dry IB strength (MPa) | 0.37 | 0.45 | 0.61 | 0.78 |
| TMA deflection ($\mu$m) | 20.9 | 21.0 | 21.0 | 20.8 |

gram trends, there also appears to be a quantitatively different relative position of the vitrification and gel curves. Thus, quantitative TTT and CHT diagrams for tannin-based adhesives cannot be generalized to all tannins, but are valid only for a particular tannin according to: (1) the chemical structure of the A-ring it presents; (2) for a particular proportion of formaldehyde hardener, which is equivalent to the effect of the variation of the molar ratio in synthetic resins, although to a much more limited extent; and (3) according to the pH used, a parameter that is more sensitive for tannins than for synthetic thermosetting adhesives.[8]

The higher-temperature zones of the CHT diagrams for the procyanidin-type pine bark tannin, at natural extraction pH of 4.8 and at pH 7, are reported in Figures 1 and 2. The marked depen-

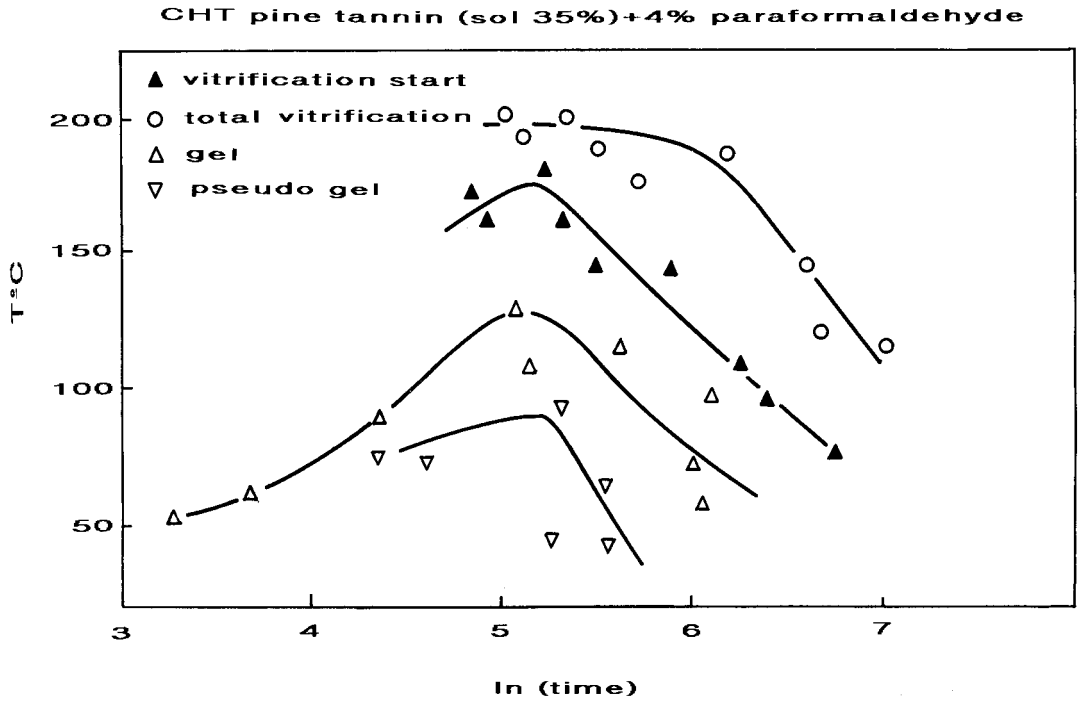


**Figure 1** Detail of the high-temperature zone of the CHT curing diagram of pine tannin extract water solution of 35% concentration, at its natural extraction pH of 4.8, hardened with 4 wt % paraformaldehyde powder. Temperature in °C, time in min.

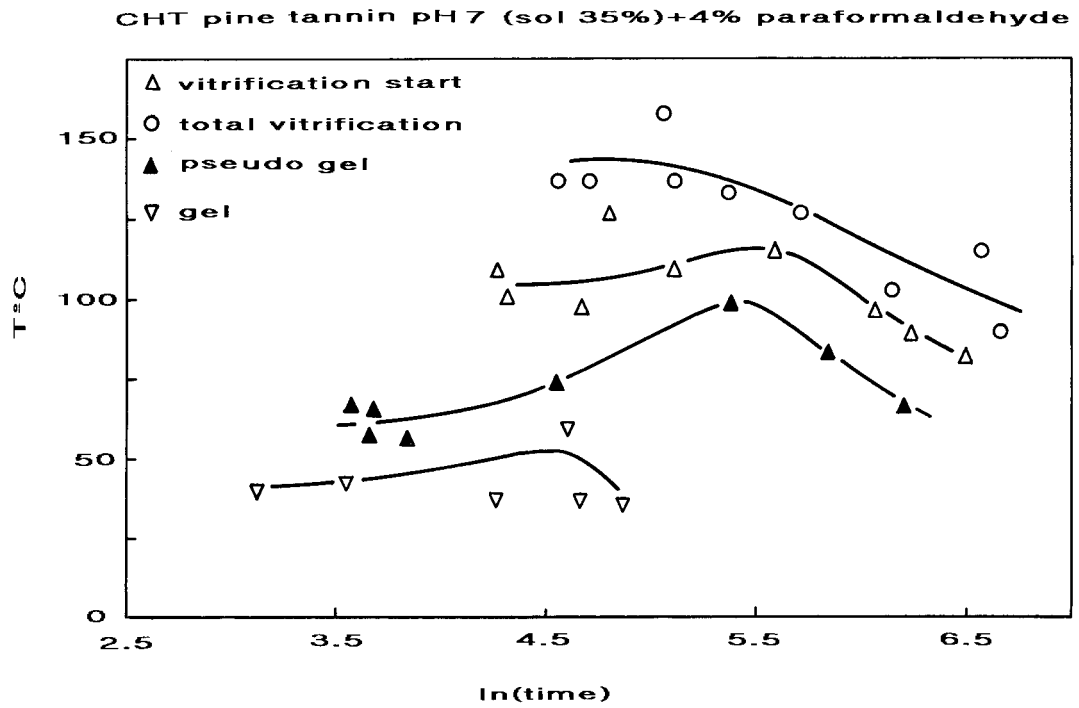


**Figure 2** Detail of the high-temperature zone of the CHT curing diagram of pine tannin extract water solution of 35% concentration, at a pH of 7, hardened with 4 wt % paraformaldehyde powder. Temperature in °C, time in min.

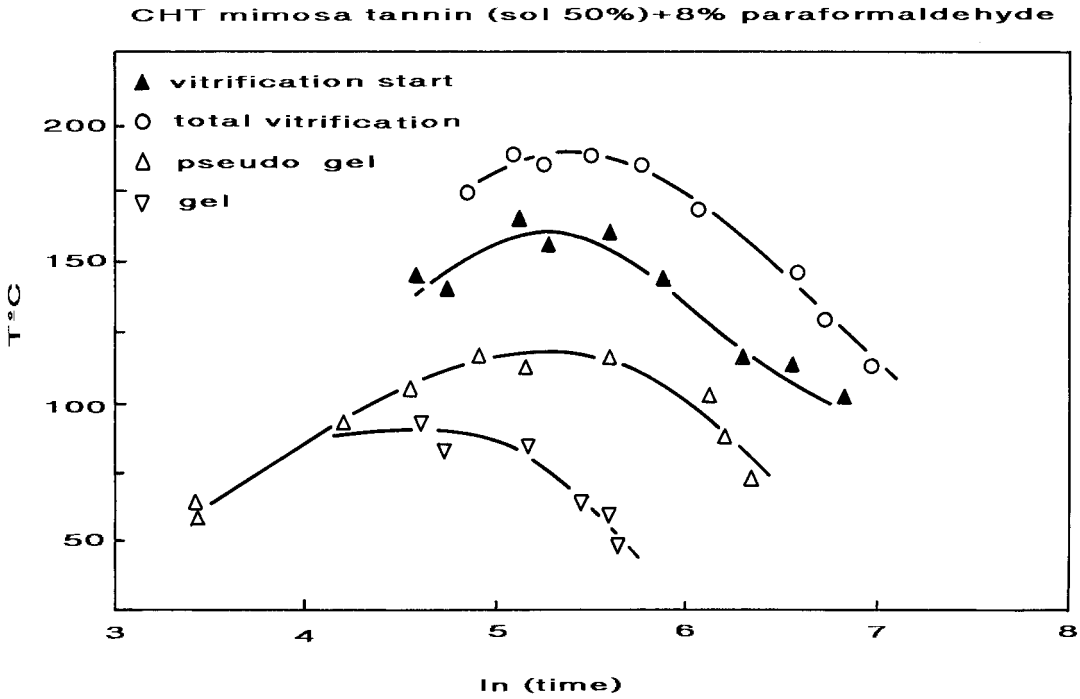


**Figure 3** Detail of the high-temperature zone of the CHT curing diagram of mimosa tannin extract water solution of 50% concentration, at its natural extraction pH of 4.2, hardened with 8 wt % paraformaldehyde powder. Temperature in °C, time in min.

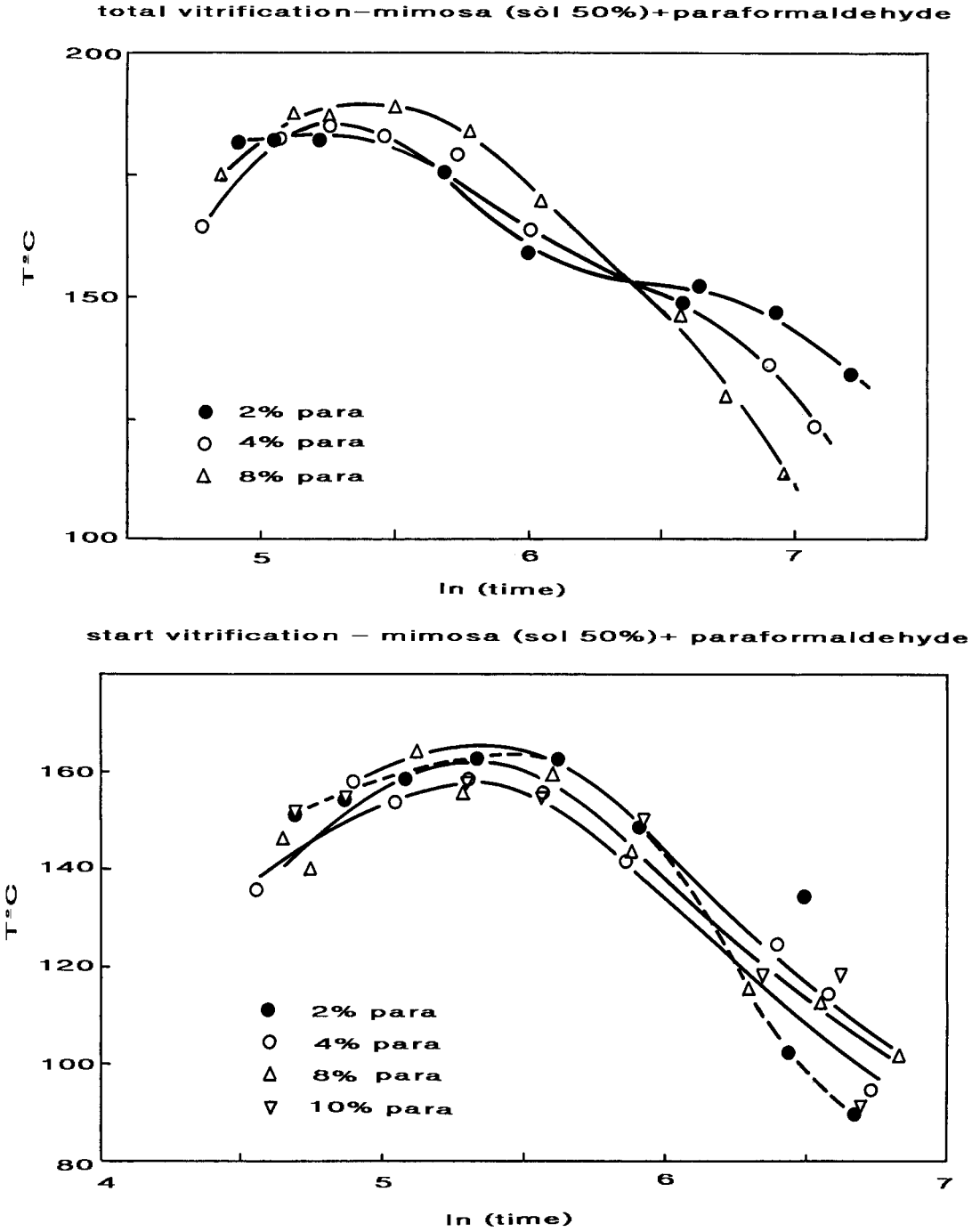


**Figure 4** Details of the variations induced in the high-temperature zone of the CHT diagram by variation of the percentage of paraformaldehyde added to a polyflavonoid tannins of the profisetinidin/prorobinetidin type: (a) total vitrification curve (mimosa), (b) start of vitrification curve (mimosa), (c) gel curve (modified quebracho). Temperature in °C, time in min.

dence on solution pH of the reaction of any tannin with formaldehyde is easily observed when comparing these two figures. For example, the maximum temperature of the gelification curve occurs at approximately 99°C for the pH 7 case and at 134°C at pH 4.8; in the latter case the gel curve inverts direction at ln time of 5, whereas in the former case it already inverted at ln time of 5.4.

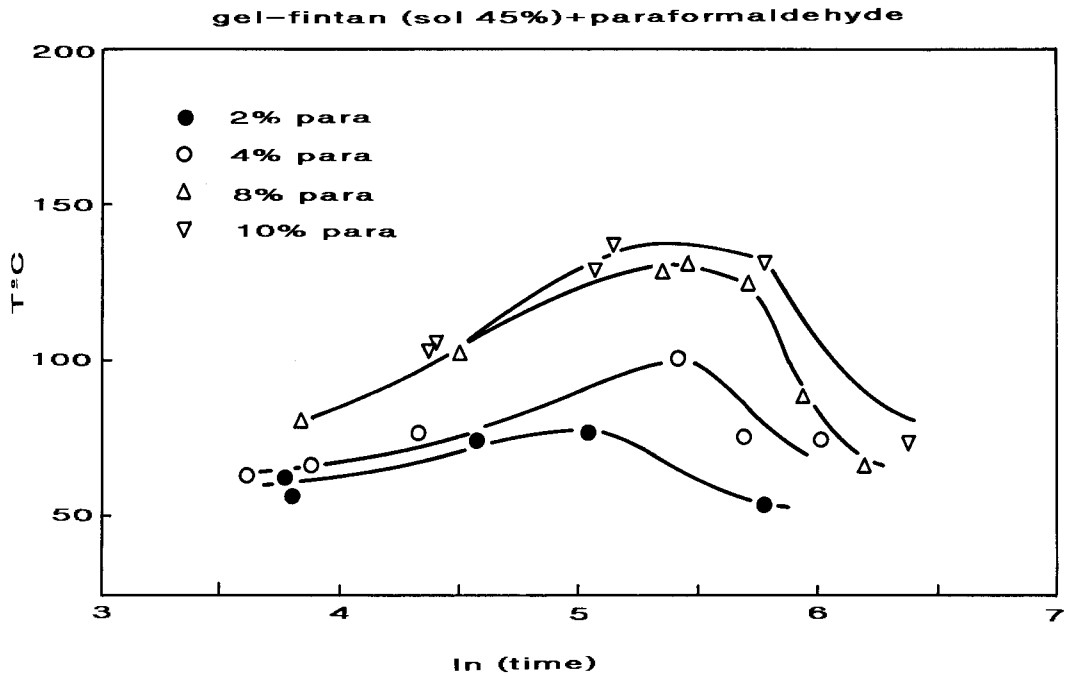


**Figure 4** (*Continued from the previous page*)

The same trend of lower temperature for a pH of higher reactivity is equally, if not even more, marked for the vitrification curves. Under identical pH conditions mimosa tannin is a much slower reacting tannin than pine tannin. A comparison of Figures 1 and 3 illustrates not only this point but also the dependence of the CHT diagram from a second parameter, the proportion of formaldehyde hardener used. In Figures 1 and 3 pine and mimosa tannins are at the same pH, at which pine is much faster reacting than mimosa, but doubling the amount of formaldehyde hardener used for mimosa yields approximately similar CHT diagrams, with the temperatures at which are situated the gel and vitrification curves of mimosa indicating that under these conditions this tannin reacts even slightly faster than pine tannin.

It must be pointed out, however, that only the slower-reacting profisetinidin/prorobinetinidin-type tannins (i.e., mimosa and quebracho) show some dependence of their CHT curing diagram on the proportion of the formaldehyde hardener used, probably because of their slower rate of curing, as illustrated in Figure 4(a)–(c). Figure 4(a) and (b) show that the dependence on the percentage of formaldehyde hardener of the start of and total vitrification curves on the CHT diagram exists but that it is not extremely marked, whereas it is much more marked in the case of the gel curves shown in Figure 4(c). The percentage of formaldehyde used is then a mostly dynamic effect, contributing more to the rate of network formation than to the tightness of the network itself. Instead, the faster-reacting tannins such as the procyanidin and prodelphinidin types induce, at any proportion of formaldehyde used, early immobilization of the network formed, with no apparent gain of strength with increases of the amount of formaldehyde hardener. This point is confirmed by the possibility (or not) to obtain regression equations that connect the TMA minimum deflection $f$ (obtained on curing a tannin with different percentages of formaldehyde hardener) with the internal bond (IB) strength of wood particleboard bonded using the same tannin/formaldehyde mix. This is possible in the case of nonmodified mimosa tannin and modified quebracho tannin but not for the faster-reacting pine and pecan tannins (Table I). Thus, in the latter two cases an increase in the percentage of formaldehyde hardener does not correspond to any noticeable increase in TMA modulus, or to any decrease in the value of the TMA minimum deflection $f$, whereas some improvement in particleboard IB strength is noticeable, even if this parameter also appears to be rather insensitive for the two faster-

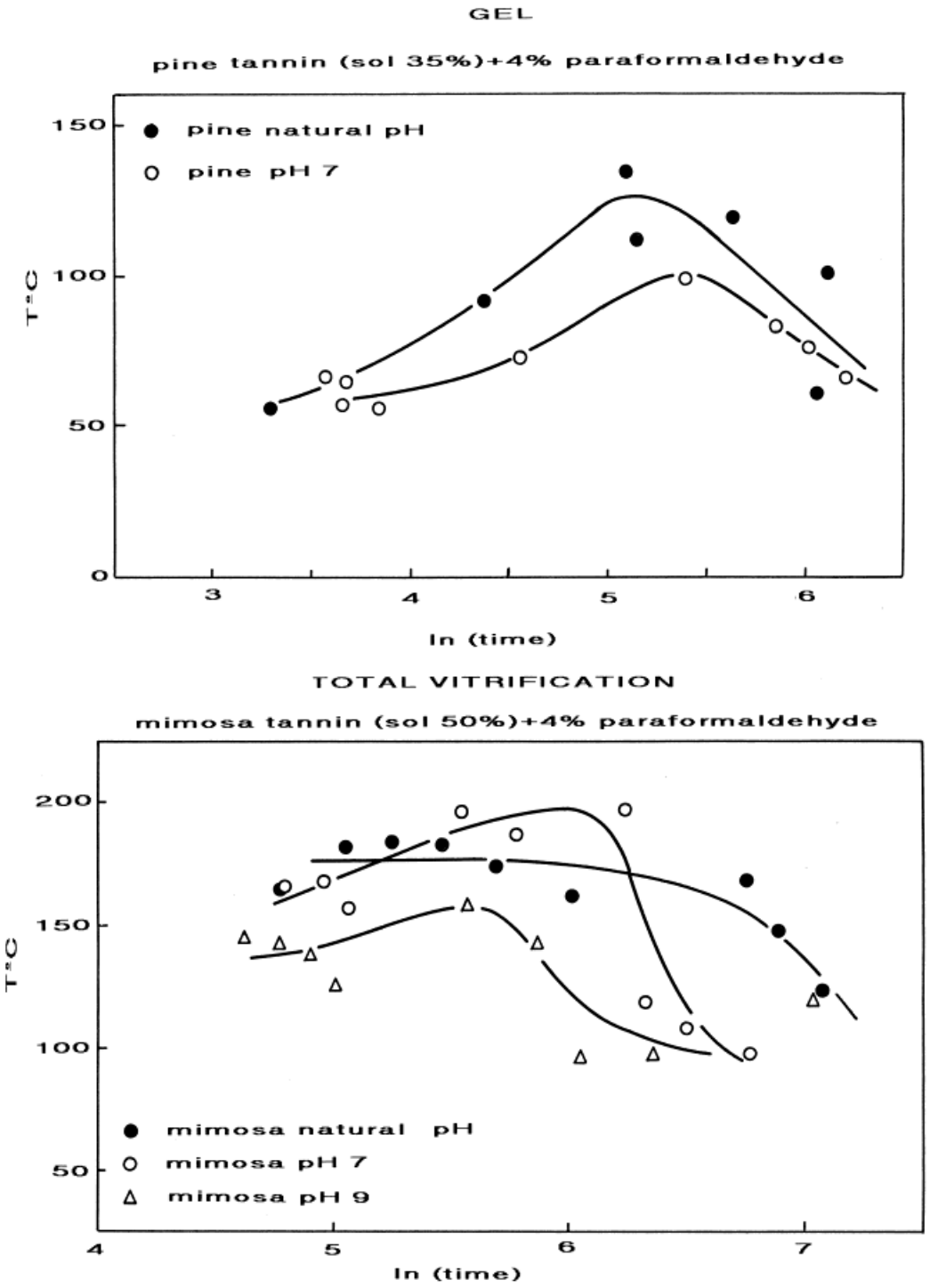


**Figure 5** Details of the variations induced in the high-temperature zone of the CHT diagram by variations of pH of polyflavonoid tannins solutions. (a) Comparison of gel curves at 4 wt % paraformaldehyde and pH 4.8 and 7 for pine tannin extract at 35% concentration in water. (b) Comparison of total vitrification curves at 4 wt % paraformaldehyde and pH 4.8, 7, and 9 for mimosa tannin extract at 50% concentration in water. Temperature in °C, time in min.

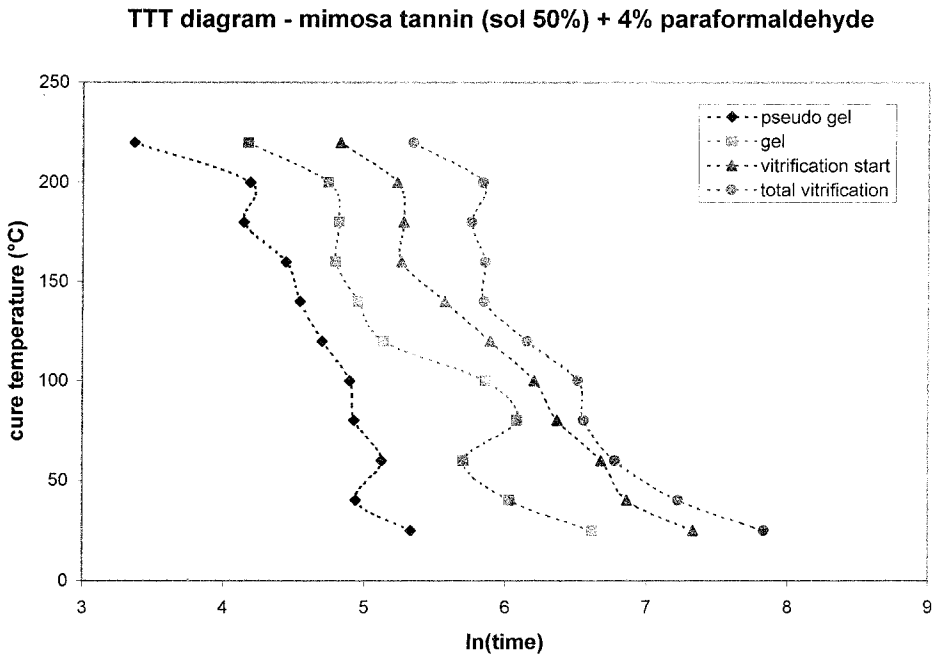


**Figure 6** Detail of the high-temperature zone of the TTT curing diagram of mimosa tannin extract water solution of 50% concentration, at its natural extraction pH of 4.2, hardened with 4 wt % paraformaldehyde powder. Temperature in °C, time in min.

reacting tannins to the variation in hardener percentage.

This is further confirmation that for higher-reactivity tannins, such as pine and pecan, the reaction with formaldehyde is so fast as to induce early immobilization of the network formed with the consequent insensitivity to the percentage of hardener used (Table I). In the case of mimosa and quebracho tannins, from the results in Table I, regression equations correlating the two parameters can be obtained, in the same manner as already presented for synthetic polycondensation resins[15–17]; that is

$$\mathrm{IB} = 38.35\ (1/f) - 1.852$$

in the case of mimosa tannin extract, the coefficient of correlation $r = 0.88$, where the IB is expressed in MPa and $f$ in $\mu$m; for modified quebracho tannin extract

$$\mathrm{IB} = 11.81\ (1/f) - 0.075$$

$r = 0.98$. Both equations are valid within the formaldehyde percentage range 4–10 wt % on tannin extract solids. In Figure 4(a)–(c) the order in which the curves at different hardener percentages occur is the same (lower to higher temperature: 2, 4, 8, and 10 wt %) for the gel [Fig. 4(c)] and the start of vitrification curves [Fig. 4(b)], whereas the same order sequence is valid only for the higher-temperature zone in the case of the total vitrification curve [Fig. 4(a)]. For the total vitrification curves the order is inverted at lower temperatures because of the common crossover point at ln time of 6.4 and temperature of 155°C [Fig. 4(a)]. These differences appear to indicate that only at the higher temperatures a greater hardener percentage leads to either (1) faster vitrification at equal temperature or (2) lower temperature of vitrification for equal time. In the case of the gel curves, at equal temperature, corresponds a slightly longer gel time, the higher is the percentage of hardener. This may appear as unexpected, but is probably the result of the type of hardener used, as polyoxymethylene (paraformaldehyde) must first depolymerize to react with the tannin.

In Figure 5(a) and (b) are shown examples of the dependence on the pH of the CHT diagram gel and total vitrification curves, respectively, for pine and mimosa tannins at a fixed hardener percentage (4 wt %), in the higher-temperature zone of the diagram. The pH, hence the rate of the tannin–formaldehyde reaction, appears to markedly influence the relative positions of the curves

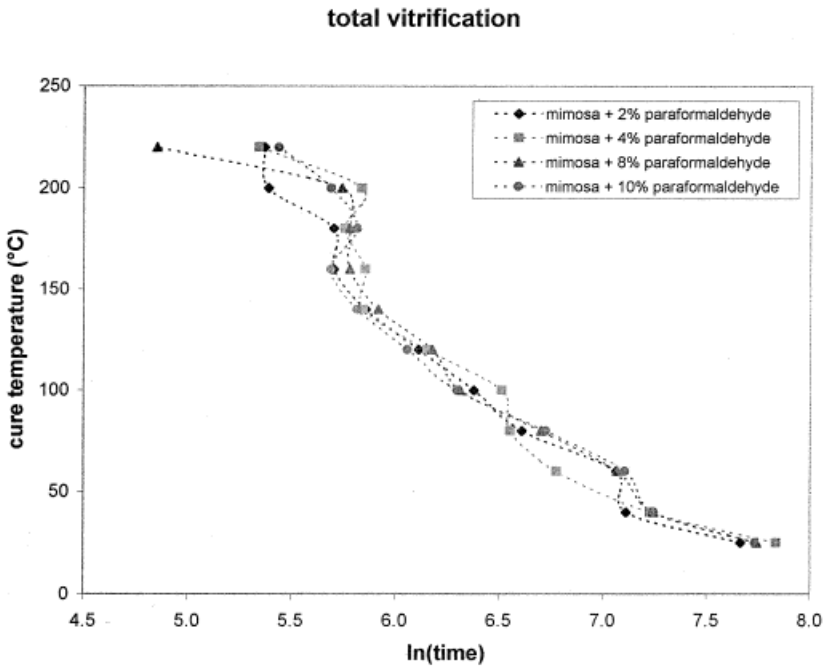


**Figure 7** Detail of the variation of the total vitrification curve high-temperature zone induced by variations in the percentage paraformaldehyde (2, 4, 8, and 10 wt %) in the TTT curing diagram of mimosa tannin extract water solution of 50% concentration, at its natural extraction pH of 4.2. Note the lack of sensitivity to the change in hardener percentage. Temperature in °C, time in min.

on the diagram, in which the higher pHs shift the position of the curves to lower temperatures, as could be expected.

The experimental TTT diagrams shown in Figure 6 for mimosa tannin show the different trend from the CHT diagrams for the same resins as previously noticed for the TTT diagrams of synthetic PF, PRF, MUF, and UF resins on wood substrates.[15–17] To start to understand the trend shown in Figure 6, it is first necessary to observe what happens to the modulus of the wood substrate alone (without the presence of a resin) when examined under the same conditions of a wood joint during bonding.[7] No significant degradation occurs up to a temperature of 180°C. Some slight degradation starts to occur at 200°C, but after some initial degradation the elastic modulus again settles to a steady value as a function of time and at a value rather comparable to the steady value obtained at lower temperatures. Evident degradation, which starts to be noticeable only in the 220–240°C range, becomes even more noticeable at higher temperatures.

The effect of substrate degradation on the TTT diagrams in Figure 6 can then only start to influence the trends in gel and vitrification curves at temperatures higher than 200°C, and it is for this reason that the region of the curves higher than 200°C are indicated by segmented lines on the figure. At a temperature $\leq$ 200°C the trends observed are attributed only to the resin. In this range of temperature the eventual turning to longer time and stable temperature of the vitrification curve, characteristic of the TTT diagrams of epoxy resins, starts to become noticeable in both vitrification and gel curves, although this trend is rapidly stopped by the start of the degradation of the substrate at 200°C (Fig. 6). Thus, the indication is that diffusion hindrance at a higher degree of conversion for these resins also becomes the determinant parameter that defines the reaction rate, before degradation of the substrate sets in and masks this trend. However, what differs from epoxy resins on glass diagrams is that the trend of all the curves (i.e., the gel curve) and the start of vitrification and end of vitrification curves are the same, as previously observed for synthetic formaldehyde-based resins.[7]

In epoxy resin TTT diagrams the trend of the gelation curve is completely different from that reported here. The result shown in Figure 6, however, is more logical because, if diffusion problems

alter the trend of the vitrification curve, then the same diffusional problem should also alter the gel curve. This is indeed what the experimental results in Figure 6 indicate. It may well be that in water-borne resins the effect is more noticeable than that in epoxy resins. With the data available and with the limitation imposed by the start of wood substrate degradation at higher temperatures, here too it is not really possible to say whether the gel curve and the vitrification curve run asymptotically toward the same value of temperature at time = $\infty$, although the indications are that this is quite likely to be the case. What is also evident in the trend of the gel curve is the bulge at about 75°C, which type of occurrence was already discussed for both gel and vitrification curves in the case of synthetic formaldehyde-based resins. This turn cannot be ascribed to substrate degradation because it occurs at too low a temperature for substrate degradation to be of any significance.[7] This bulge and the changing of its occurrence can be attributed to: (1) movements of water coming from the substrate toward the resin layer, to ease the diffusional problem already proved to occur in these materials even at moderate degrees of conversion[4]; and (2) initial diffusional problems resulting either from early entanglements,[7,12,18] as a consequence of the particular bulkiness of tannin oligomers, or from the rapid formation and subsequent internal rearrangements of methylene–ether–bridged loose networks, which are well known to occur in all phenolic resins, including those that are tannin based.[12,18]

Figure 7 shows the experimental points obtained for the TTT curing diagram vitrification curves of mimosa tannin at different percentages of formaldehyde hardener being added. It is evident that in TTT diagrams the variation in the percentage of formaldehyde hardener influences even less the relative position and trend of the curve than that observed in CHT diagrams [Fig. 4(a)–(c)]. Figure 7 clearly indicates that in the TTT diagram these parameters appear to have no influence at all.

## CONCLUSIONS

To conclude, TTT and CHT curing diagrams for tannin-based adhesives can also be built by following the *in situ* hardening directly in a wood joint and the curve trends observed are similar to those that have already been observed for synthetic polycondensation resins on lignocellulosic substrates. Of the parameters that appear to most influence the relative position of vitrification and gel curves on the diagrams, chief among them is the reactivity of the tannin with formaldehyde and any factor influencing it: thus, the inherent higher reactivity of the A-ring of the tannin (such as in procyanidins versus prorobinetinidins) and the pH of the tannin solution. The percentage formaldehyde hardener has some influence in CHT diagrams, especially for the slower-reacting tannins, but practically no influence in TTT diagrams within the 4–10% formaldehyde range used. As in the case of synthetic polycondensation adhesive resins, regression equations relating the internal bond strength of a wood particleboard, prepared under controlled conditions, with the inverse of the minimum deflection, obtained by constant heating rate TMA of a wood joint during resining cure, have been obtained for the two lower-reactivity tannins but not for the faster-reacting procyanidin and prodelphinidin tannins.

## REFERENCES


1. Enns, J. B.; Gillham, J. K. J Appl Polym Sci 1983, 28, 2831.
2. Wisanrakkit, G.; Gillham, J. K.; Enns, J. B. J Appl Polym Sci 1990, 41, 1895.
3. Montserrat, S. J Appl Polym Sci 1992, 44, 545.
4. Nunez, L.; Fraga, F.; Nunez, M. R.; Villanueva, M. J Appl Polym Sci 1998, 70, 1931.
5. Hofmann, K.; Glasser, W. G. Thermochim Acta 1990, 166, 169.
6. Pizzi, A.; Lu, X.; Garcia, R. J Appl Polym Sci 1999, 71, 915.
7. Pizzi, A.; Zhao, C.; Kamoun, C.; Heinrich, H. J Appl Polym Sci 2001, 80, 2128.
8. Pizzi, A. Wood Adhesives Chemistry and Technology; Marcel Dekker: New York, 1983.
9. Pizzi, A. J Appl Polym Sci 1997, 63, 603.
10. Pizzi, A. J Appl Polym Sci 1997, 65, 1843.
11. Pizzi, A.; Probst, F.; Deglise, X. J Adhes Sci Technol 1997, 11, 573.
12. Garcia, R.; Pizzi, A. J Appl Polym Sci 1998, 70, 1111.
13. Lu, X.; Pizzi, A. Holz Roh Werkstoff 1998, 56, 339.
14. Pascault, J. P.; Williams, R. J. J Polym Sci Phys Ed 1990, 28, 85.
15. Laigle, Y.; Kamoun, C.; Pizzi, A. Holz Roh Werkstoff 1998, 56, 154.
16. Zhao, C.; Garnier, S.; Pizzi, A. Holz Roh Werkstoff 1998, 56, 402.
17. Kamoun, C.; Pizzi, A. Holz Roh Werkstoff 2000, 58, 288.
18. Garcia, R.; Pizzi, A. J Appl Polym Sci 1998, 70, 1083.